atomic displacements in a crystal. Qualitative interpretations of the continuous diffuse scattering in terms of waves of displacement propagating along molecular filaments in tropomyosin (Boylan & Phillips, 1986), correlated rigid-body displacements in lysosyme (Doucet & Benoit, 1987), and atomic displacements and range of coupling in insulin (Caspar, Clarage, Salunke & Clarage, 1988) have been put forward previously. We have developed a more general quantitative approach to the refinement of correlated inter- and intramolecular displacements from diffuse-scattered intensities of molecular crystals (Moss & Harris, 1991). An estimate of the thermal vibration mean-square amplitudes for typical protein crystals has been made using estimates of the longitudinal speed of sound from laser-generated ultrasound measurements and of the transverse speed from Youngs modulus estimates (Edwards *et al.*, 1990).

The acoustic diffuse scattering peaks at the Bragg positions and many constitute a significant source of errors in the integrated intensity measurements. We have exploited the characteristic fine collimation of synchrotron radiation in the collection of data in which the acoustic scattering contributions are minimized to assess the effect on model refinement (I. D. Glover, D. S. Moss, J. R. Helliwell and coworkers, in preparation) and data that allow the modelling of the acoustic diffuse scattering. We have shown that at low resolutions at least the scattering may be explained in terms of one-phonon interactions and that, in principle, the form of the phonon-scattering factors may be extracted from these measurements.

We are grateful to the Science and Engineering Research Council, Birkbeck College and the Universities of Keele, York and Manchester for the support of this work, the Director and Staff at the SERC Daresbury Laboratory for the provision of synchrotron radiation, and to Professor P. Sigler, Dr D. Rice and Dr M. Adams for the provision of experimental data relating to t-RNA(Met), GDH and 6-PGDH respectively.

References

Adams, M. J., Helliwell, J. R. & Bugg, C. E. (1977). *J. Mol. Biol.* **112**, 183–197.

Al-Hilal, D., Baker, E., Carlisle, C. H., Gorinsky, B. A., Horsburgh, R. C., Lindley, P. F., Moss, D. S., Schneider, H. & Stimpson, R. (1976). *J. Mol. Biol.* **108**, 255–257.

Boylan, D. & Phillips, G. N. Jr (1986). *Biophys. J.* **49**, 76–78.

Carlisle, C. H., Lindley, P. F., Moss, D. S. & Slingsby, C. (1977). *J. Mol. Biol.* **110**, 417–419.

Carlisle, C. H., Palmer, R. A., Mazumdar, S. I., Gorinsky, B. A. & Yeates, D. G. R. (1974). *J. Mol. Biol.* **85**, 1–18.

Caspar, D. L. D., Clarage, J., Salunke, D. M. & Clarage, M. (1988). *Nature (London)*, **352**, 659–662.

Doucet, J. & Benoit, J. P. (1987). *Nature (London)*, **325**, 643–646.

Edwards, C., Palmer, S. B., Emsley, P., Helliwell, J. R., Glover I. D., Harris, G. W. & Moss, D. S. (1990). *Acta Cryst.* A**46**, 315–320.

Moss, D. S. & Harris, G. W. (1991). *Acta Cryst.* In preparation

Nave, C., Helliwell, J. R., Moore, P. R., Thompson, A. W., Worgan, J. S., Greenall, R. J., Miller, A., Bentley, S. K., Bradshaw, J., Pigram, W. J., Fuller, W., Siddons, D. P., Deutsh, M. & Tregear, R. T. (1985). *J. Appl. Cryst.* **18**, 396–401.

Rice, D. W., Hornby, D. P. & Engel, P. C. (1985). *J. Mol. Biol.* **181**, 147–149.

Wood, S. P., Pitts, J. E., Blundell, T. L. & Jenkins, J. A. (1977). *Eur. J. Biochem.* **78**, 119–126.

Acta Cryst. (1991). B**47**, 968–975

Disordered Fatty-Acid Chains in Piperazinium Myristate and Palmitate

By L. Venkatramani and B. M. Craven

Department of Crystallography, University of Pittsburgh, Pittsburgh, PA 15260, *USA*

(*Received* 1 *February* 1991; *accepted* 18 *June* 1991)

Abstract

(I) Piperazinium *n*-tetradecanoate (myristate), $C_4H_{12}N_2^{2+}.2C_{14}H_{27}O_2^-$, $M_r = 542{\cdot}85$, m.p. = 368·9 K, triclinic, $P\bar{1}$, $a = 5{\cdot}681\ (1)$, $b = 7{\cdot}454\ (1)$, $c = 20{\cdot}676\ (3)$ Å, $\alpha = 84{\cdot}59\ (1)$, $\beta = 86{\cdot}37\ (1)$, $\gamma = 81{\cdot}73\ (1)^\circ$, $V = 861{\cdot}5$ Å^3, $Z = 1$, $T = 296$ K, $D_m = 1{\cdot}05$, $D_x = 1{\cdot}05$ g cm^{-3}, $F(000) = 304$, Mo $K\alpha$, $\lambda = 0{\cdot}7107$ Å, $\mu = 0{\cdot}723$ cm^{-1}, $R = 0{\cdot}062$ for 2198 independent reflections with $I > \sigma(I)$. (II) Piperazinium *n*-hexadecanoate (palmitate), $C_4H_{12}N_2^{2+}.2C_{16}H_{31}O_2$, $M_r = 598{\cdot}95$, m.p. = 370·2 K, triclinic, $P\bar{1}$, $a = 5{\cdot}678\ (1)$, $b = 7{\cdot}472\ (1)$, $c = 22{\cdot}916\ (3)$ Å, $\alpha = 84{\cdot}64\ (1)$, $\beta = 89{\cdot}82\ (1)$, $\gamma = 81{\cdot}32\ (1)^\circ$, $V = 956{\cdot}8$ Å^3, $Z = 1$, $T = 296$ K, $D_m = 1{\cdot}04$, $D_x = 1{\cdot}04$ g cm^{-3}, $F(000) = 336$, Mo $K\alpha$, $\lambda = 0{\cdot}7107$ Å, $\mu = 0{\cdot}708$ cm^{-1}, $R = 0{\cdot}052$ for 1931 independent reflections with $I > \sigma(I)$. These crystal structures, together with the previously reported *n*-decanoate and *n*-dodecanoate (laurate) salts, form an isostructural series. The piperazinium cations, which have a crystallographic centre of symmetry, are in

0108-7681/91/060968-08$03.00

the chair conformation. Each cation forms a salt bridge to four different anions with N···O distances ranging from 2·67 to 2·70 Å. The alkanoate chains are bent with torsion angles of 78·6° (I) and 79·7° (II) at the C3—C4 bond. The longer sections of the alkanoate chains are close-packed together in an antiparallel array. The C2—C3 bonds, occurring between the carboxylate group and the bend in the chain, are apparently very short [1·476 (8) Å in (I) and 1·434 (9) Å in (II)]. These distances involve the mean positions of atoms which are disordered. Bimodal probability density functions are obtained for atoms C2 and C3 when a Gram–Charlier expression with fourth-order terms is assumed for the mean-square displacement of these atoms. In this region of the chain, two slightly different conformations occur with equal probability.

Introduction

In proposing a scheme for indentifying and isolating alkanoic acids, it was reported by Pollard, Adelson & Bain (1934) that the piperazine salts of these acids readily give large well-formed crystals. We have found this to be true for a number of long-chain fatty acids which otherwise would be difficult to obtain as crystals suitable for X-ray and neutron structural study. We began by preparing the piperazinium laurate, myristate and palmitate salts which we crystallized as large plates.* Here we report the crystal structure determinations of piperazinium myristate and palmitate which are isostructural with the decanoate and laurate salts earlier reported by Sangin & Brisse (1984) and Brisse & Sangin (1982). Unexpectedly, we find that at room temperature, the myristate and palmitate chains are disordered with respect to small conformational differences localized between the carboxylate group and the fourth carbon atom, which is where the chain bends. For the two C atoms most affected, the disorder has been treated by including the fourth-order terms of the Gram–Charlier series in the expression for the mean-square atomic displacements (Johnson & Levy, 1974; Kuhs, 1983). It is likely that a similar disorder occurs in the corresponding decanoate and laurate structures.

Experimental

Crystals of the two salts were obtained by slow evaporation from methanol (myristate) or isopropanol (palmitate). Crystal densities were measured by flotation in chloroform/benzene. Melting points were obtained and a search for possible crystal phase transitions was carried out using a Mettler TA-3000 system for differential scanning calorimetry. Both salts underwent a low-temperature phase transition (267 K, $\Delta H = 4{\cdot}4$ kJ mol^{-1} for myristate; 254 K, $\Delta H = 3{\cdot}2$ kJ mol^{-1} for palmitate). Although efforts were made to collect diffractometer intensity data for structure determination of the low-temperature phases, they were unsuccessful because of crystal damage caused during the phase transition. Nevertheless, it was established that the low-temperature phases are triclinic.* Thus the structure determinations were carried out only for the high-temperature phases, using X-ray data collected at room temperature.

The diffraction data were measured with crystals of dimensions 0·5 × 0·4 × 0·4 mm (myristate) and 0·5 × 0·3 × 0·4 mm (palmitate) using an Enraf–Nonius CAD-4 diffractometer and Nb-filtered Mo $K\alpha$ radiation. Unit-cell dimensions were obtained by least-squares fit of 25 reflections with $15 < \theta < 25°$. Integrated intensities were collected by $\omega/2\theta$ scans for reflections having $\sin\theta/\lambda < 0{\cdot}60$ Å^{-1} and reflection indices in the range h from 0 to 6, k from -8 to 8 and l from -24 to 24. Three monitor reflections showed no significant intensity variations. For the myristate (palmitate), the total number of reflections measured was 3278 (3717). No absorption corrections were applied. After averaging of equivalents [$R_{\rm int} = 0{\cdot}006$ (0·009)], there were 3004 (2856) independent reflections including 2198 (1931) with $I > \sigma(I)$. Only the latter were included in the structure determination. The phases were determined by direct methods using the *MITHRIL* computer program (Gilmore, 1983) and the initial structure refinements were by full-matrix least squares using the *SHELX*76 programs (Sheldrick, 1976). The function minimized was $\sum w(|F_o| - |F_c|)^2$ with $w = \sigma^{-2}$. Atomic scattering factors were taken from Cromer & Waber (1965) for C, N, O and Stewart, Davidson & Simpson (1965) for H. Mean-square displacement parameters were refined anisotropically for C, N and O atoms, isotropically for H (located in a difference Fourier synthesis). Final values for myristate (palmitate) were $wR = 0{\cdot}053$ (0·047), with maximum $\Delta/\sigma = 0{\cdot}04$ (0·08). Final atomic positional and mean-square atomic displacement parameters are given in Table 1(a).† Interatomic distances and angles are given in

---

* For the palmitate salt, typical crystal dimensions were 3·0 × 1·7 × 0·5 mm, mass 2·8 mg.

* At 246 K, myristate: $a = 5{\cdot}65$, $b = 7{\cdot}48$, $c = 20{\cdot}08$ Å, $\alpha = 97{\cdot}0$, $\beta = 94{\cdot}6$, $\gamma = 96{\cdot}8°$; palmitate: $a = 5{\cdot}65$, $b = 7{\cdot}42$, $c = 22{\cdot}04$ Å, $\alpha = 97{\cdot}0$, $\beta = 91{\cdot}2$, $\gamma = 97{\cdot}2°$. Rotation photographs and diffractometer searches gave no indication of axial doubling at low temperature.

† Tables of reflection data, positional and thermal parameters for H atoms, and molecular dimensions involving H atoms have been deposited with the British Library Document Supply Centre as Supplementary Publication No. SUP 54357 (43 pp.). Copies may be obtained through The Technical Editor, International Union of Crystallography, 5 Abbey Square, Chester CH1 2HU, England.

Table 1. *Atomic parameters*

(*a*) Positional and mean-square anisotropic displacement parameters for piperazinium myristate (above) and piperazinium palmitate (below) with e.s.d.'s in parentheses. Entries with only one line (C15, C16) are for palmitate. Entries for C2* and C3* are from the refinement assuming harmonic atomic displacements for all atoms. Entries for C2 and C3 are the U^{ij} values in the final refinement where these two atoms were also assigned fourth-order displacements. The anisotropic displacement factors have the form $T_2 = \exp[-2\pi^2\sum_i\sum_j h_ih_ja^{*i}a^{*j}U^{ij}]$.

	x	y	z	U^{11}	U^{22}	U^{33}	U^{12}	U^{13}	U^{23}
N(1*P*)	0·5108 (5)	0·1851 (4)	0·9731 (2)	0·0210 (19)	0·0333 (21)	0·0561 (28)	0·0043 (15)	0·0039 (17)	0·0045 (19)
	−0·5169 (8)	0·1852 (6)	0·9759 (2)	0·0226 (34)	0·0319 (28)	0·0575 (34)	0·0045 (23)	0·0050 (24)	0·0019 (24)
C(1*P*)	0·4293 (8)	0·0332 (6)	0·9328 (2)	0·0414 (29)	0·0518 (28)	0·0387 (34)	0·0128 (22)	0·0013 (25)	−0·0036 (24)
	−0·4439 (11)	0·0345 (8)	0·9399 (3)	0·0374 (45)	0·0572 (43)	0·0447 (43)	−0·0086 (32)	0·0005 (33)	0·0005 (33)
C(2*P*)	−0·4610 (8)	0·1340 (6)	1·0424 (2)	0·0326 (28)	0·0384 (28)	0·0514 (28)	−0·0050 (23)	0·0006 (22)	0·0074 (22)
	−0·4533 (10)	0·1328 (7)	1·0378 (3)	0·0291 (40)	0·0356 (36)	0·0590 (42)	−0·0027 (29)	0·0044 (31)	−0·0110 (31)
O1	0·0206 (5)	0·2625 (4)	0·9553 (2)	0·0298 (16)	0·0492 (20)	0·0823 (26)	−0·0079 (14)	−0·0067 (16)	0·0243 (18)
	0·0115 (6)	0·2615 (5)	0·9597 (2)	0·0259 (24)	0·0500 (25)	0·0859 (31)	0·0057 (18)	0·0013 (19)	0·0238 (22)
O2	0·2821 (5)	0·4601 (4)	0·9194 (2)	0·0262 (16)	0·0458 (20)	0·0929 (26)	−0·0054 (14)	−0·0004 (16)	0·0147 (18)
	0·3009 (6)	0·4599 (5)	0·9278 (2)	0·0198 (24)	0·0491 (25)	0·1061 (34)	−0·0038 (19)	0·0034 (21)	0·0172 (22)
C1	0·0629 (7)	0·4009 (6)	0·9209 (2)	0·0304 (26)	0·0402 (28)	0·0607 (33)	0·0088 (21)	0·0011 (23)	0·0030 (24)
	0·0822 (11)	0·4024 (7)	0·9293 (2)	0·0367 (43)	0·0448 (38)	0·0626 (42)	0·0167 (32)	0·0021 (32)	0·0030 (31)
C2*	0·1079 (9)	0·5014 (8)	0·8756 (3)	0·0313 (29)	0·0680 (41)	0·1115 (56)	−0·0132 (28)	−0·0024 (33)	0·0293 (39)
	0·0774 (13)	0·5027 (11)	0·8891 (4)	0·0227 (51)	0·0771 (59)	0·1602 (95)	−0·0093 (41)	−0·0028 (54)	0·0572 (63)
C2				0·0284 (37)	0·0808 (60)	0·1123 (72)	0·0228 (37)	0·0133 (40)	0·0377 (52)
				0·0169 (60)	0·0681 (61)	0·2003 (133)	0·0041 (41)	0·0106 (61)	0·0775 (72)
C3*	0·0272 (9)	0·6896 (8)	0·8492 (3)	0·0468 (31)	0·0709 (39)	0·0687 (41)	0·0150 (28)	−0·0010 (29)	0·0191 (33)
	0·0043 (12)	0·6849 (10)	0·8643 (3)	0·0586 (50)	0·0964 (58)	0·0677 (57)	0·0255 (42)	0·0009 (45)	0·0282 (45)
C3				0·0517 (47)	0·0995 (72)	0·0604 (51)	0·0314 (46)	−0·0119 (38)	0·0376 (49)
				0·0474 (69)	0·1304 (95)	0·0676 (59)	0·0348 (58)	0·0126 (45)	0·0552 (64)
C4	0·2124 (10)	0·7717 (9)	0·8044 (3)	0·0594 (38)	0·0769 (46)	0·0651 (44)	0·0252 (34)	0·0011 (31)	0·0147 (36)
	0·1723 (13)	0·7689 (10)	0·8241 (3)	0·0630 (57)	0·0926 (63)	0·0596 (52)	−0·0267 (48)	0·0055 (42)	0·0154 (44)
C5	0·2364 (10)	0·7125 (9)	0·7366 (3)	0·0616 (37)	0·0768 (50)	0·0590 (41)	0·0304 (35)	0·0020 (31)	0·0026 (35)
	0·1820 (13)	0·7108 (10)	0·7631 (3)	0·0578 (54)	0·0973 (64)	0·0604 (53)	0·0328 (48)	0·0010 (43)	0·0118 (45)
C6	0·4306 (10)	0·7833 (8)	0·6927 (3)	0·0587 (36)	0·0658 (43)	0·0563 (38)	−0·0214 (31)	−0·0010 (29)	0·0031 (31)
	0·3651 (13)	0·7853 (10)	0·7237 (3)	0·0596 (55)	0·0764 (57)	0·0629 (52)	−0·0190 (46)	0·0028 (44)	0·0008 (43)
C7	0·4539 (10)	0·7207 (9)	0·6255 (3)	0·0619 (40)	0·0721 (47)	0·0631 (43)	−0·0234 (35)	−0·0047 (32)	0·0018 (35)
	0·3743 (13)	0·7243 (10)	0·6630 (3)	0·0665 (57)	0·0826 (60)	0·0663 (55)	−0·0270 (49)	0·0004 (45)	0·0017 (46)
C8	0·6518 (10)	0·7850 (8)	0·5811 (3)	0·0618 (36)	0·0687 (42)	0·0573 (38)	0·0200 (31)	0·0002 (29)	−0·0045 (30)
	0·5654 (13)	0·7873 (10)	0·6236 (3)	0·0630 (55)	0·0774 (55)	0·0585 (50)	0·0191 (45)	0·0063 (42)	0·0071 (42)
C9	0·6726 (10)	0·7193 (8)	0·5143 (3)	0·0636 (40)	0·0708 (43)	0·0577 (30)	−0·0207 (34)	0·0068 (31)	−0·0019 (33)
	0·5722 (13)	0·7223 (10)	0·5637 (3)	0·0628 (56)	0·0801 (57)	0·0629 (51)	0·0254 (45)	0·0014 (45)	0·0008 (43)
C10	0·8693 (10)	0·7831 (8)	0·4698 (3)	0·0609 (37)	0·0704 (44)	0·0590 (40)	0·0162 (32)	0·0012 (31)	−0·0109 (32)
	0·7630 (13)	0·7827 (10)	0·5240 (3)	0·0646 (55)	0·0777 (56)	0·0606 (51)	0·0183 (46)	0·0022 (44)	−0·0117 (42)
C11	0·8867 (10)	0·7166 (8)	0·4028 (3)	0·0623 (37)	0·0708 (42)	0·0548 (37)	−0·0193 (32)	−0·0033 (30)	0·0077 (31)
	0·7697 (13)	0·7194 (10)	0·4637 (3)	0·0635 (53)	0·0777 (53)	0·0575 (50)	−0·0231 (43)	−0·0023 (42)	0·0039 (41)
C12	1·0828 (10)	0·7822 (8)	0·3578 (3)	0·0618 (37)	0·0798 (44)	0·0540 (39)	−0·0191 (33)	0·0003 (30)	−0·0141 (33)
	0·9581 (13)	0·7810 (10)	0·4235 (3)	0·0649 (58)	0·0761 (57)	0·0652 (54)	0·0184 (46)	0·0005 (46)	0·0161 (43)
C13	1·0999 (11)	0·7100 (9)	0·2917 (3)	0·0756 (44)	0·0875 (50)	0·0600 (42)	0·0243 (38)	0·0057 (34)	0·0107 (36)
	0·9632 (13)	0·7173 (10)	0·3635 (3)	0·0662 (57)	0·0797 (57)	0·0570 (51)	−0·0223 (47)	−0·0008 (44)	0·0087 (42)
C14	1·2943 (14)	0·7750 (11)	0·2457 (3)	0·1008 (61)	0·1306 (69)	0·0696 (51)	−0·0386 (53)	0·0161 (45)	−0·0248 (50)
	1·1509 (13)	0·7799 (10)	0·3236 (3)	0·0676 (58)	0·0827 (58)	0·0598 (52)	0·0165 (48)	0·0017 (45)	−0·0119 (43)
C15	1·1549 (19)	0·7122 (11)	0·2638 (3)	0·0853 (65)	0·0988 (69)	0·0638 (56)	−0·0309 (56)	0·0054 (49)	−0·0086 (49)
C16	1·3410 (17)	0·7735 (13)	0·2230 (4)	0·1020 (79)	0·1297 (86)	0·0757 (67)	−0·0269 (71)	0·0207 (63)	−0·0242 (63)

(*b*) Fourth-order displacement parameters ($d^{ijkl} \times 10^n$) given by the expression: $T_4 = 2\cdot 3\pi^4\sum_i\sum_j\sum_k\sum_l h_ih_jh_kh_l d^{ijkl}$. Columns headed *M* and *P* refer to the myristate and palmitate structures.

		C2	C3	C2	C3
ijkl	*n*	*M*	*M*	*P*	*P*
1111	8	−15 (13)	14 (20)	31 (37)	−12 (46)
2222	8	15 (11)	77 (19)	−18 (9)	109 (32)
3333	7	3 (3)	2 (1)	22 (7)	1 (1)
1112	8	7 (7)	26 (11)	9 (11)	32 (17)
1222	8	14 (7)	−44 (12)	7 (6)	28 (17)
1113	8	−7 (3)	−8 (3)	8 (5)	−11 (4)
1333	7	−5 (4)	−2 (2)	18 (7)	−1 (2)
2223	8	4 (2)	18 (4)	10 (3)	29 (6)
2333	7	5 (4)	1 (23)	25 (8)	7 (3)
1122	8	5 (6)	25 (10)	−2 (6)	12 (13)
1133	7	5 (8)	2 (7)	12 (12)	8 (7)
2233	7	17 (7)	16 (7)	36 (15)	44 (11)
1123	7	30 (15)	66 (20)	47 (20)	48 (24)
1223	7	40 (15)	99 (22)	−16 (18)	113 (29)
1233	7	17 (6)	8 (5)	25 (9)	−17 (7)

Table 2. Fig. 1 shows the configuration of the molecules in the asymmetric unit, together with the atomic nomenclature and anisotropic mean-square displacement ellipsoids. Fig. 2 shows the molecular packing and hydrogen bonding.

At this stage, it was noted that the C2—C3 bonds in both structures appeared to be significantly shorter [1·476 (8) and 1·434 (9) Å] than the average length [1·507 (8) Å] obtained for the other 26 C—C bonds. It seemed unlikely that this apparent bond shortening was real. Therefore, we expected that an analysis of the thermal vibrations of the chains in terms of rigid-body motion (Schomaker & Trueblood, 1968) together with internal torsional modes (Dunitz & White, 1973) might provide considerable librational corrections for the C2—C3 bond lengths. However, in our analysis using programs by Craven, He & Weber (1986), we obtained bond-lengthening corrections of only 0·004 and 0·003 Å. We recognize that a model in which the chains are rigid is only an approximation. At the other extreme, we have considered the approximation in which C2 and C3 vibrate independently of each other (Busing & Levy, 1964). The corrected C2—C3 bond lengths then become 1·576 and 1·565 Å. These calculations indicate that there might exist a model of intermediate character involving correlated harmonic vibrations of C2 and C3 whereby the C2—C3 bond lengths could be suitably explained. Alternatively, the explanation might come from considering a disorder of the chains in the region of C2 and C3.

We calculated a Fourier and difference Fourier synthesis of the electron density in sections through C2 and also through C3. We were unable to interpret these maps (Fig. 3) in terms of atomic disorder. However, there were remarkable similarities in the corresponding maps for the myristate and palmitate structures, indicating that the residual features were

Table 2. *Interatomic distances* (Å) *and angles* (°)

The distances and angles given for C2* and C3* are for the average positions of the atoms which are disordered.

	Uncorrected		Corrected for thermal libration	
	Myristate	Palmitate	Myristate	Palmitate
O1—C1	1·249 (5)	1·254 (7)	1·258	1·266
O2—C1	1·261 (5)	1·251 (7)	1·278	1·270
C1—C2*	1·530 (7)	1·517 (10)		
C2*—C3*	1·476 (8)	1·434 (10)		
C3*—C4	1·515 (9)	1·525 (10)		
C4—C5	1·501 (9)	1·500 (10)	1·503	1·502
C5—C6	1·507 (9)	1·510 (10)	1·507	1·510
C6—C7	1·499 (9)	1·502 (10)	1·500	1·503
C7—C8	1·509 (9)	1·511 (10)	1·510	1·511
C8—C9	1·501 (8)	1·497 (10)	1·502	1·500
C9—C10	1·504 (8)	1·507 (10)	1·505	1·507
C10—C11	1·508 (8)	1·500 (10)	1·509	1·502
C11—C12	1·512 (8)	1·506 (10)	1·512	1·507
C12—C13	1·508 (8)	1·495 (10)	1·509	1·500
C13—C14	1·514 (10)	1·502 (10)	1·515	1·502
C14—C15		1·503 (11)		1·505
C15—C16		1·504 (12)		1·504
N(1*P*)—C(1*P*)	1·473 (6)	1·467 (8)		
N(1*P*)—C(2*P*)	1·482 (6)	1·467 (8)		
C(1*P*)—C(2*P*′)	1·506 (6)	1·505 (9)		

	Myristate	Palmitate
O1—C1—O2	123·9 (4)	124·0 (5)
O1—C1—C2*	118·6 (4)	118·0 (5)
O2—C1—C2*	117·5 (4)	117·9 (5)
C1—C2*—C3*	119·0 (5)	120·4 (6)
C2*—C3*—C4	113·5 (4)	115·0 (6)
C3*—C4—C5	115·4 (5)	114·8 (6)
C4—C5—C6	116·0 (5)	115·4 (6)
C5—C6—C7	115·2 (5)	114·8 (6)
C6—C7—C8	116·4 (5)	116·1 (6)
C7—C8—C9	115·4 (5)	114·9 (6)
C8—C9—C10	115·6 (5)	115·6 (6)
C9—C10—C11	114·9 (5)	115·9 (6)
C10—C11—C12	114·9 (5)	116·2 (6)
C11—C12—C13	113·8 (5)	115·8 (6)
C12—C13—C14	114·6 (6)	115·5 (6)
C13—C14—C15		114·6 (6)
C14—C15—C16		115·6 (7)
C(1*P*)—N(1*P*)—C(2*P*)	111·5 (3)	111·4 (5)
N(1*P*)—C(2*P*)—C(1*P*′)	110·5 (4)	110·8 (5)
N(1*P*)—C(1*P*)—C(2*P*′)	111·3 (4)	111·5 (5)
O1—C1—C2—C3	−162·8 (5)	164·9 (6)
O2—C1—C2—C3	19·7 (7)	18·8 (10)
C1—C2—C3—C4	−179·2 (5)	−179·2 (6)
C2—C3—C4—C5	78·6 (7)	79·7 (8)
C3—C4—C5—C6	176·2 (5)	177·0 (6)
C4—C5—C6—C7	179·2 (5)	179·4 (6)
C5—C6—C7—C8	−178·2 (5)	−176·5 (6)
C6—C7—C8—C9	179·5 (5)	179·2 (6)
C7—C8—C9—C10	179·9 (5)	179·5 (6)
C8—C9—C10—C11	179·7 (5)	179·5 (6)
C9—C10—C11—C12	179·4 (5)	179·3 (6)
C10—C11—C12—C13	178·6 (5)	180·0 (6)
C11—C12—C13—C14	179·6 (5)	179·8 (6)
C12—C13—C14—C15		179·2 (7)
C13—C14—C15—C16		179·9 (7)
N(1*P*)—C(1*P*)—C(2*P*′)—N(1*P*′)	−55·6 (5)	55·4 (6)
N(1*P*)—C(2*P*)—C(1*P*′)—N(1*P*′)	55·6 (5)	55·4 (6)
C(1*P*)—N(1*P*)—C(2*P*)—C(1*P*′)	−55·7 (4)	−55·3 (6)
C(2*P*)—N(1*P*)—C(1*P*)—C(2*P*′)	56·1 (5)	55·7 (6)
C(2*P*′)—N(1*P*′)—C(1*P*′)—C(2*P*)	−56·1 (5)	−55·7 (6)
C(1*P*′)—N(1*P*′)—C(2*P*′)—C(1*P*)	55·7 (5)	55·3 (6)

Hydrogen-bond interactions (myristate above, palmitate below)

X—H···*Y*	*X*—H (Å)	H···*Y* (Å)	*X*···*Y* (Å)	*X*—H···*Y* (°)
N(1*P*)—H(1*NP*)···O2^{i}	0·99 (4)	1·73 (4)	2·698 (5)	164 (3)
	1·03 (3)	1·68 (3)	2·695 (6)	167 (3)
N(1*P*)—H(2*NP*)···O1^{ii}	0·87 (4)	1·84 (4)	2·683 (5)	162 (4)
	0·99 (3)	1·68 (3)	2·672 (6)	173 (3)

van der Waals distances (Å)†

	Myristate	Palmitate
O2···H(22*P*)	2·33 (3)	2·35 (3)
C1···H(2*NP*)	2·73 (3)	2·56 (4)

Symmetry code: (i) x, y, z; (ii) $x-1, y, z$.

† O···H < 2·6, C···H < 2·9 Å.

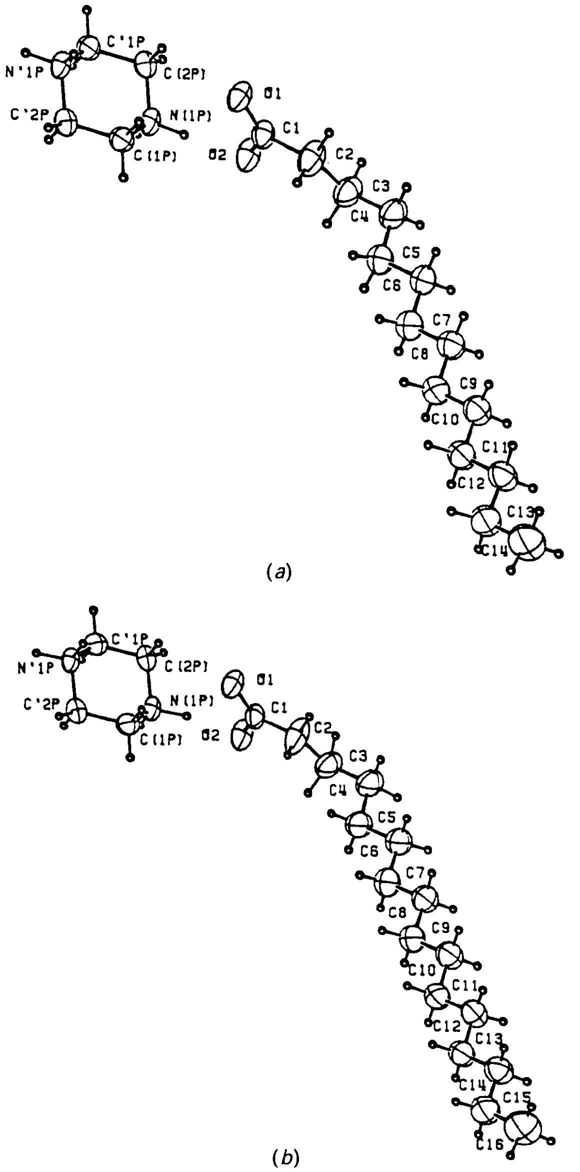

Fig. 1. Atomic nomenclature and mean-square displacement ellipsoids at the 50% probability level (Johnson, 1976). The anions are shown for the ordered average structure as obtained in the initial structure refinement. (*a*) Piperazinium myristate. (*b*) Piperazinium palmitate.

not the result of random errors in the data. Additional refinements were carried out with the *POP* system of computer programs (Craven, Weber & He, 1987), making use of the Gram–Charlier expansion to include higher-order terms in the expression for the mean-square atomic displacements. Initially, the set of ten third-order (c^{jkl}) and fifteen fourth-order (d^{ijkl}) terms were included for all O and C atoms from the carboxylate group through to C4. Subsequently, the third-order displacement parameters for all atoms were omitted. These terms, which describe the skewness of the probability density function (p.d.f.) of each nucleus, were strongly correlated with the corresponding atomic positional parameters. Our inability to determine whether the atomic p.d.f.'s are actually skewed is attributed to the limited resolution of the available diffraction data ($\sin\theta/\lambda < 0{\cdot}60$ Å^{-1}). Also, we found that fourth-order terms were insignificantly different from zero, except for C2 and C3. In the final cycles of refinement, there were 43 variables consisting of an overall scale factor and U^{ij} and d^{ijkl} for atoms C2 and C3 only. Other parameters for all atoms, including C2 and C3, were fixed with values obtained from the original refinement which assumed harmonic atomic mean-square displacements. For the myristate (palmitate) refinements, there was a reduction in wR from 0·053 to 0·050 (0·047 to 0·045) and the goodness of fit became $S = 2{\cdot}18$ (1·74). The improvement in agreement can be accepted at the 99·5% level of confidence (Hamilton, 1974). The

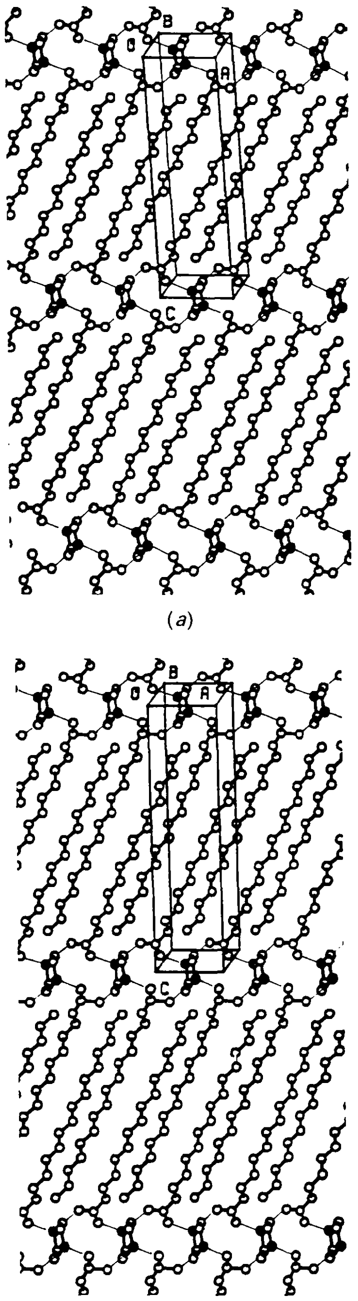

(*a*)

(*b*)

Fig. 2. Crystal packing and hydrogen bonding. Piperazinium nitrogen atoms are shown as solid circles. (*a*) Piperazinium myristate. (*b*) Piperazinium palmitate.

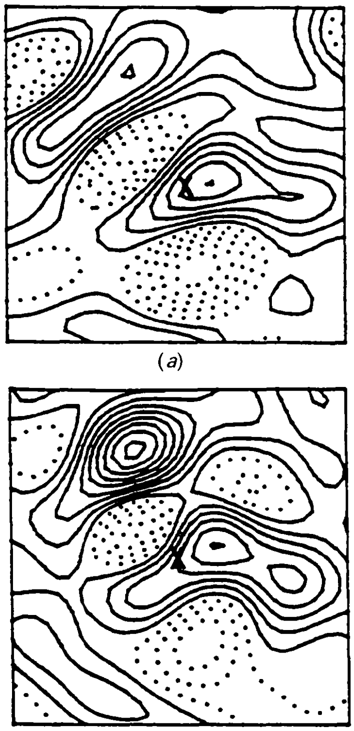

(*a*)

(*b*)

Fig. 3. Difference Fourier synthesis showing the residual electron density at C2 after the initial structure refinement. The section is in the plane which bisects the angle C1—C2—C3. The projection of the chain backbone is across the page. Contours are at intervals of 0·05 e Å^{-3}. Each map is shown for an area 1 × 1 Å. (*a*) Piperazinium myristate. (*b*) Piperazinium palmitate.

Table 3. *Thermal vibration analysis for the alkanoate anions*

The anions are assumed to be vibrating as segmented rigid bodies. The model assumes overall rigid-body vibrations (Schomaker & Trueblood, 1968) with internal libration about the C1···C4 axis as described by Dunitz & White (1973). Disordered atoms C2 and C3 were omitted from the least-squares fit of atomic U^{ij}. Fitting was carried out with the Cartesian crystal axes *a*, *b**, *a* × *b**, and with the origin at the center of mass of the anion.

	Myristate			Palmitate		
Goodness of fit		2·153			1·893	
R.m.s. value for $[(U^{ij})_{\rm obs} - (U^{ij})_{\rm calc}]$, excluding H atoms		0·00071 Å^2			0·00068 Å^2	
wR		0·123			0·142	
Ω† (deg^2)		75 (17)			96 (20)	
Translational tensor, **T** (Å^2 × 10^3)	44 (5)	5 (3)	−1 (3)	46 (5)	−7 (4)	−3 (3)
		68 (3)	6 (2)		81 (4)	5 (3)
			59 (2)			62 (3)
Mean-square principal values, **T** (Å^2)	0·043	0·072	0·056	0·045	0·084	0·061
Librational tensor, **L** (deg^2)	3·1 (17)	1·1 (9)	−6·0 (28)	3·3 (18)	0·4 (8)	−6·4 (30)
		0·9 (5)	0·8 (15)		0·7 (4)	−0·2 (15)
			10·7 (52)			9·2 (55)
Mean-square principal values, **L** (deg^2)	0·4	1·1	14·1	−0·8	0·7	13·3
Cross tensor (deg Å × 10^3)	8 (15)	−2 (7)	10 (5)	13 (18)	4 (8)	6 (6)
	7 (1)	−5 (10)	2 (2)	−8 (1)	−4 (11)	3 (2)
	27 (14)	24 (14)	3	−32 (17)	7 (16)	−9

† Torsional libration about the C1···C4 axis.

final anisotropic displacement parameters for C2 and C3 are given in Table 1(*a*) and the fourth-order parameters are presented in Table 1(*b*). The atomic displacement parameters in Table 1(*a*) were used to obtain molecular thermal vibrational parameters (Table 3) which in turn were used to obtain corrected bond lengths for the alkanoate chains (Table 2).

The p.d.f.'s for C2 and C3 shown in Fig. 4 were obtained using computer programs by Craven, He & Weber (1986). For both atoms, the p.d.f. is elongated with an indication that the distribution is bimodal. Because we omitted the third-order terms from the Gram Charlier expansion, the resulting p.d.f.'s have a center of symmetry. We interpret these p.d.f.'s in

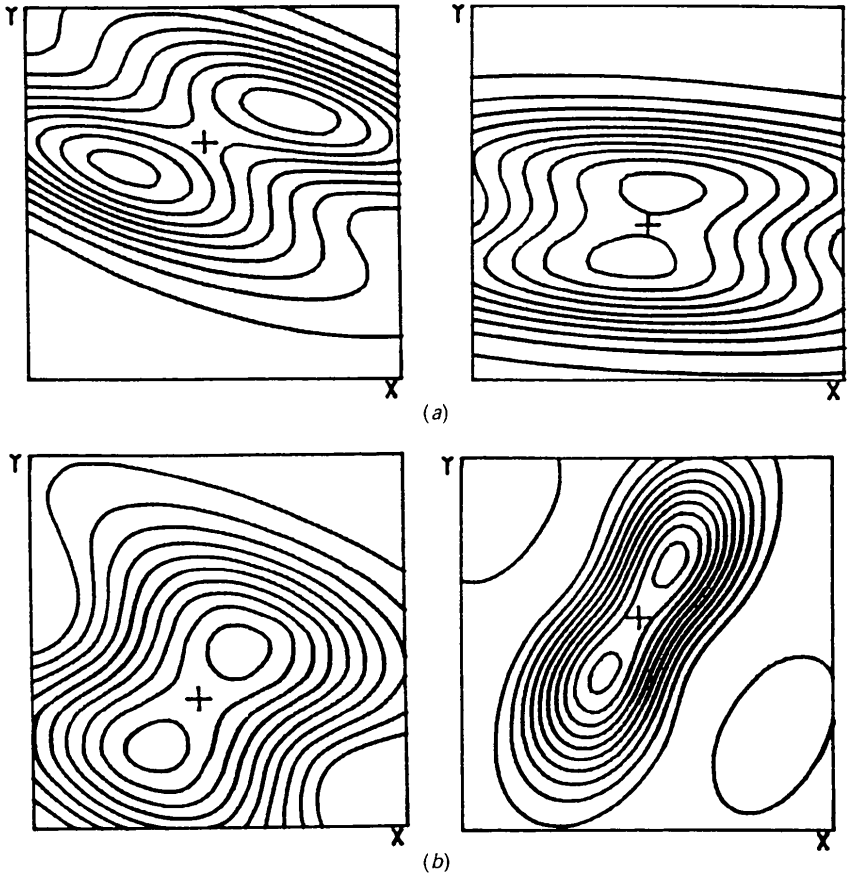

Fig. 4. Total probability density functions (p.d.f.'s) for atoms C2 and C3. The p.d.f. for the myristate anion is shown on the left and for the palmitate on the right. Contours are at equal arbitrary intervals. Each p.d.f. is shown for an area of 1 × 1 Å. (*a*) Section through C2 in the plane bisecting the angle C1—C2—C3. (*b*) Section through C3 in the plane bisecting the angle C2—C3—C4.

terms of disorder of both C2 and C3 with respect to two alternate sites occupied with equal probability. The positional parameters for these sites are shown in Table 4. The separations of alternate sites are 0·21 and 0·15 Å for C2 and C3 respectively in the myristate structure and 0·18 and 0·17 Å in the palmitate structure. The distances and angles involving alternate sites (Table 4) are consistent with the alkanoate chain existing as two conformers *a* and *b* which differ in the region of C2 and C3.

Table 4. *Atomic parameters involving disordered* C2 *and* C3

Atomic nomenclature and interatomic distances and angles are labelled *a* and *b* referring to the conformers existing in each crystal structure.

Atomic positional coordinates for disordered sites of C2 and C3 in piperazinium myristate and piperazinium palmitate

	Myristate			Palmitate		
	x	*y*	*z*	*x*	*y*	*z*
C2*a*	0·1169	0·5035	0·8801	0·0937	0·4932	0·8914
C2*b*	0·0967	0·4995	0·8722	0·0705	0·4961	0·8861
C3*a*	0·0287	0·6918	0·8517	0·0016	0·6775	0·8632
C3*b*	0·0118	0·6951	0·8462	0·0019	0·6939	0·8676

Distances (Å) and angles (°) for disordered atoms

	Myristate		Palmitate	
	a	*b*	*a*	*b*
C1—C2	1·53	1·52	1·52	1·51
C2—C3	1·50	1·53	1·49	1·49
C3—C4	1·53	1·53	1·51	1·51
O1—C1—C2	116	121	114	119
O2—C1—C2	119	115	122	117
C1—C2—C3	117	119	116	119
C2—C3—C4	113	110	116	113
C3—C4—C5	117	113	113	119
O1—C1—C2—C3	165	−162	169	−155
O2—C1—C2—C3	13	24	14	32
C1—C2—C3—C4	172	174	179	180
C2—C3—C4—C5	80	80	83	69
C3—C4—C5—C6	176	180	175	−177

Discussion

In both crystal structures, the piperazinium cation, which has a crystallographic center of symmetry, is in the chair conformation. Ring-puckering coordinates (Q, θ, φ) as defined by Cremer & Pople (1975) are (0·556, 0, 0) in the myristate salt and (0·549, 0, 0) in the palmitate, corresponding to a ring slightly flatter than for an ideal cyclohexane molecule (Q = 0·63). Bond distances and angles for the cation are normal (Table 3). The four N—H groups of each cation form a hydrogen bond with a carboxylate O atom of a different alkanoate anion having N···O distances in the range 2·672 (6) to 2·698 (5) Å. As is to be expected for N—H···O interactions in which both N and O carry a formal charge, the N···O distances are on the short side of the distribution reported by Taylor, Kennard & Versichel (1984). Except for a bend at the C3—C4 bond, the alkanoate chains are almost fully extended, as can be seen from Fig. 1 and the backbone torsion angles (Table 2). The shorter chain sections and the carboxylate groups pack with the piperazinium cations (Fig. 2). The longer chain sections pack with each other in an antiparallel arrangement. Other views of the packing and hydrogen bonding are shown by Brisse & Sangin (1982) for the isostructural laurate salt. In the longer chain sections, variations in C—C distances (1·495 to 1·514 Å) and C—C—C angles (113·8 to 116·4°) are at most marginally significant in terms of the experimental errors. However, the distances are systematically too short and the angles too large when compared with the values 1·526 (2) Å and 112·4 (2)° obtained for propane by Lide (1960) from microwave data. We attribute these differences to the effect of thermal vibrations in the crystal. However, the corrections are difficult to estimate for long fatty-acid chains particularly in the present case where the atomic displacements involve both thermal motion and disorder.

For the disordered chain conformers *a* and *b*, the distances and angles involving C2 and C3 (Table 4) are chemically reasonable but they are not accurately determined. Probably, the adjacent carboxylate atoms and C4 also have slightly different positions in *a* and *b* but for these atoms, the higher-order displacement terms were insignificant so that bond distances and angles necessarily involve their averaged atomic positions. We do not understand why the molecular packing for the myristate and palmitate structures at room temperature allows disorder with two slightly different chain conformers. However, the disordered model provides an explanation for the apparent shortness of the C2—C3 bond lengths and is also consistent with our observation that there are phase transitions occurring at 267 and 254 K for the myristate and palmitate salts respectively. The structural changes at the transition must be small because the changes in the unit-cell dimensions and in the enthalpy (4·4 and 3·2 kJ mol^{-1}) are small. We believe that in the low-temperature phases, the structures are ordered. One possibility is that the conformers *a* and *b* persist. The crystallographic center of symmetry is lost so that the low-temperature structures have space group $P1$ with two formula units in the unit cell. We consider it more likely that the cooling of these structures gives rise to contraction which is associated with a slightly different, more efficient, chain packing in which conformers *a* and *b* become indistinguishable. The space group would remain $P\bar{1}$.

For the isostructural piperazinium decanoate and dodecanoate structures determined at room temperature, Sangin & Brisse (1984) and Brisse & Sangin (1982), reported unusually short C2—C3 bond lengths [1·453 (4), 1·460 (9) Å]. They did not consider the possibility of chain disorder. We have not extended our study to these shorter chain members in the series, but the apparent shortness of the C2—C3 bonds indicates that at room temperature, all four related structures are disordered in a similar way.

This work was supported by grant HL-20350 from the National Institutes of Health. We are grateful to Dr R. Shiono for the use of computer programs and also to Dr John Ruble and Mrs Joan Klinger for technical assistance.

References

BRISSE, F. & SANGIN, J.-P. (1982). *Acta Cryst.* **B38**, 215–221.

BUSING, W. R. & LEVY, H. A. (1964). *Acta Cryst.* **17**, 142–146.

CRAVEN, B. M., HE, X. M. & WEBER, H.-P. (1986). *Programs for Thermal Motion Analysis* (updated). Tech. Rep. Department of Crystallography, Univ. of Pittsburgh, USA.

CRAVEN, B. M., WEBER, H.-P. & HE, X. M. (1987). *The POP Refinement Procedure*. Tech. Rep. Department of Crystallography, Univ. of Pittsburgh, USA.

CREMER, D. & POPLE, J. A. (1975). *J. Am. Chem. Soc.* **97**, 1354–1358.

CROMER, D. T. & WABER, J. T. (1965). *Acta Cryst.* **18**, 104–109.

DUNITZ, J. D. & WHITE, D. N. J. (1973). *Acta Cryst.* **A29**, 93–94.

GILMORE, C. G. (1983). *MITHRIL. Computer Program for the Automatic Solution of Crystal Structures from X-ray Data*. Univ. of Glasgow, Scotland.

HAMILTON, W. A. (1974). *International Tables for X-ray Crystallography*, Vol. IV, p. 288. Birmingham: Kynoch Press. (Present distributor Kluwer Academic Publishers, Dordrecht.)

JOHNSON, C. K. (1976). *ORTEPII*. Report ORNL-5138. Oak Ridge National Laboratory, Tennessee, USA.

JOHNSON, C. K. & LEVY, H. A. (1974). *International Tables for X-ray Crystallography*, Vol. IV, p. 316. Birmingham: Kynoch Press. (Present distributor Kluwer Academic Publishers, Dordrecht.)

KUHS, W. F. (1983). *Acta Cryst.* **A39**, 148–158.

LIDE, D. R. (1960). *J. Chem. Phys.* **33**, 1514–1518.

POLLARD, C. B., ADELSON, D. E. & BAIN, J. P. (1934). *J. Am. Chem. Soc.* **56**, 1759–1760.

SANGIN, J.-P. & BRISSE, F. (1984). *Acta Cryst.* **C40**, 2094–2096.

SCHOMAKER, V. & TRUEBLOOD, K. N. (1968). *Acta Cryst.* **B24**, 63–76.

SHELDRICK, G. M. (1976). *SHELX*. Program for crystal structure determination. Univ. of Cambridge, England.

STEWART, R. F., DAVIDSON, E. R. & SIMPSON, W. T. (1965). *J. Chem. Phys.* **42**, 3175–3187.

TAYLOR, R., KENNARD, O. & VERSICHEL, W. (1984). *Acta Cryst.* **B40**, 280–288.

Acta Cryst. (1991). **B47**, 975–986

Structure of Porcine Insulin Cocrystallized with Clupeine Z

BY P. BALSCHMIDT AND F. BENNED HANSEN

Novo-Nordisk A/S, Niels Steensensvej 1, 2820 *Gentofte, Denmark*

AND E. J. DODSON, G. G. DODSON AND F. KORBER*

*Department of Chemistry, University of York, York YO*1 5*DD, England*

(*Received* 19 *September* 1989; *accepted* 9 *July* 1991)

Abstract

The crystal structure of NPH-insulin, pig insulin cocrystallized with zinc, *m*-cresol and protamine, has been solved by molecular replacement and refined using restrained least-squares refinement methods. The final crystallographic *R* factor for all reflections between 2 and 10 Å is 19·4%. The insulin molecules are arranged as hexamers with two tetrahedrally coordinated Zn atoms in the central channel and one *m*-cresol bound to each monomer near His *B*5. One protamine binding site has been unequivocally identified near a dimer–dimer interface, although most of the polypeptide is crystallographically disordered. The conformation of the insulin moiety and the structural differences between the three unique monomers have been analysed. The zinc and *m*-cresol environments are described and the nature of the protamine binding site is outlined.

Introduction

Microcrystalline preparations of insulin cocrystallized with protamines, basic polypeptides of the cell nucleus which are rich in arginine and lysine, (NPH-insulin) were obtained as long as 40 years ago (Krayenbuhl & Rosenberg, 1946) and have been used successfully in the treatment of diabetes ever since. Owing to its slow release properties after subcutaneous injection, protamine–insulin has been a very popular pharmaceutical formulation. Our aim is to investigate how this delayed action is brought about, how and to what extent the protamine is incorporated into the crystal structure, and to find and describe possible changes in the insulin structure in this particular crystal form. Preliminary data from two different structural studies on salmine–insulin have been reported (Baker & Dodson, 1970; Eggena, Magdoff-Fairchild, Rudko, Fullerton & Low, 1969; Simkin, Cole, Ozawa, Magdoff-Fairchild, Eggena, Rudko & Low, 1969; Fullerton & Low, 1970),

---

* To whom all correspondence should be addressed.

0108-7681/91/060975-12$03.00